
How Attentive are Graph Attention Networks?

Shaked Brody

Technion, Israel

shakedbr@cs.technion.ac.il

Uri Alon

Technion, Israel

urialon@cs.technion.ac.il

Eran Yahav

Technion, Israel

yahave@cs.technion.ac.il

Abstract

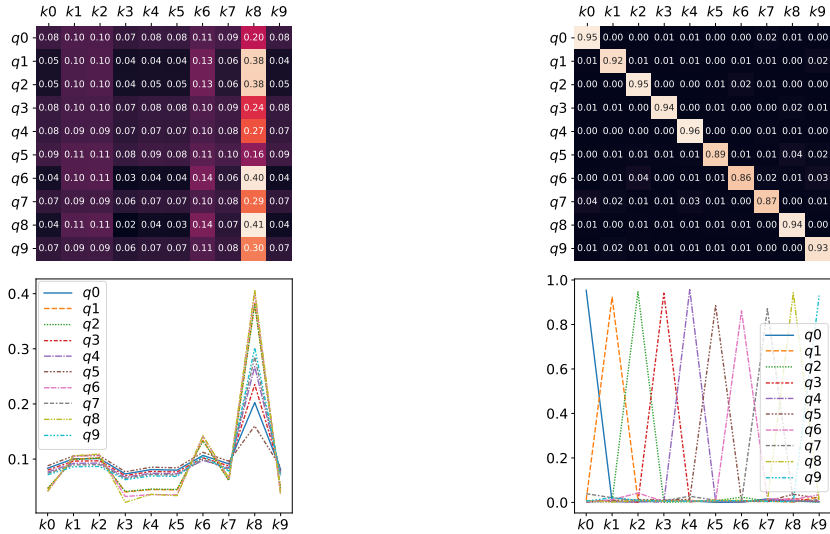
Graph Attention Networks (GATs) are one of the most popular GNN architectures and are considered as the state-of-the-art architecture for representation learning with graphs. In GAT, every node attends to its neighbors given its own representation as the query. However, in this paper we show that GATs can only compute a restricted kind of attention where the ranking of attended nodes is *unconditioned on the query node*. We formally define this restricted kind of attention as *static* attention and distinguish it from a strictly more expressive *dynamic* attention. Because GATs use a *static* attention mechanism, there are simple graph problems that GAT cannot express: in a controlled problem, we show that static attention hinders GAT from even fitting the training data. To remove this limitation, we introduce a simple fix by modifying the order of operations and propose GATv2: a *dynamic* graph attention variant that is strictly more expressive than GAT. We perform an extensive evaluation and show that GATv2 outperforms GAT across 11 OGB and other benchmarks while we match their parametric costs. Our code is available at https://github.com/tech-srl/how_attentive_are_gats.

1 Introduction

Graph neural networks (GNNs; Gori et al., 2005; Scarselli et al., 2008) have seen increasing popularity over the past few years (Duvenaud et al., 2015; Atwood and Towsley, 2016; Bronstein et al., 2017; Monti et al., 2017). GNNs provide a general and efficient framework to learn from graph-structured data. Thus, GNNs are easily applicable in domains where the data can be represented as a set of nodes and the prediction depends on the relationships (edges) between the nodes. Such domains include molecules, social networks, product recommendation, computer programs and more.

A GNN can be viewed as a message-passing network (Gilmer et al., 2017), where each node iteratively updates its state by interacting with its neighbors. GNN variants (Wu et al., 2019; Xu et al., 2019; Li et al., 2016) mostly differ in how each node aggregates the representations of its neighbors and combines them with its own representation. Veličković et al. (2018) pioneered the use of attention-based neighborhood aggregation, in one of the most popular GNN variants – Graph Attention Network (GAT). In GAT, every node updates its representation by attending to its neighbors using its own representation as the query. This generalizes the standard averaging or max-pooling of neighbors (Kipf and Welling, 2017; Hamilton et al., 2017), by allowing every node to compute a *weighted* average of its neighbors. The work of Veličković et al. also generalizes the Transformer’s (Vaswani et al., 2017) self-attention mechanism, from sequences to graphs (Joshi, 2020).

While GAT is one of the most popular GNN architectures (Bronstein et al., 2021) and is considered as the state-of-the-art neural architecture for learning with graphs (Wang et al., 2019a), we show that *GATs do not actually compute dynamic attention*, a fact that severely hinders their expressiveness. Instead, we show that GAT only uses a restricted “static” form of attention: for every query node, attention is *monotonic* with respect to its neighbor key scores. That is, the ranking (the *argsort*) of attention coefficients is shared across all nodes in the graph, and is unconditioned on the query node. This limitation of the standard GAT is demonstrated in Figure 1a.



(a) Attention in standard GAT (Veličković et al. (2018)) (b) Attention in GATv2, our fixed version of GAT

Figure 1: Standard GAT (Figure 1a) computes *static* attention: the ranking of attention coefficients is global for all nodes in the graph, and is unconditioned on the query node. For example, all queries (q_0 to q_9) attend mostly to the 8th key (k_8). In contrast, GATv2 (Figure 1b) can actually compute *dynamic* attention, where every query has a different ranking of attention coefficients of the keys.

Supposedly, the conceptual idea of attention as the form of interaction between GNN nodes is orthogonal to the specific choice of attention function. However, Veličković et al.’s original design of GAT has spread to a variety of domains (Wang et al., 2019a; Qiu et al., 2018; Yang et al., 2020; Wang et al., 2019c; Huang and Carley, 2019; Ma et al., 2020; Kosaraju et al., 2019; Nathani et al., 2019; Wu et al., 2020; Zhang et al., 2020) and has become the default implementation of “graph attention network” in all popular GNN libraries such as PyTorch Geometric (Fey and Lenssen, 2019), DGL (Wang et al., 2019b), and others (Dwivedi et al., 2020; Gordić, 2020; Brockschmidt, 2020).

To overcome the limitation we identified in GAT, we introduce a simple fix to its attention function by modifying the order of internal operations. The result is GATv2 – a graph attention variant that has a universal approximator attention function, and is thus *strictly more expressive than GAT*. The effect of fixing the attention function in GATv2 is demonstrated in Figure 1b.

In summary, our main contribution is identifying that one of the most popular GNN types, the graph attention network, cannot actually compute dynamic attention. We introduce formal definitions for analyzing the expressive power of graph attention mechanisms (Definitions 3.1 and 3.2), and derive our claims theoretically (Theorem 1) from the equations of Veličković et al. (2018). Empirically, we use a synthetic problem to show that standard GAT *cannot express* alignment problems that require *dynamic* attention (Section 4.1). We introduce a simple fix by switching the order of internal operations in the attention function of GAT, and propose GATv2, which does compute dynamic attention (Theorem 2). We further conduct a thorough empirical comparison of GAT and GATv2 and find that GATv2 outperforms GAT across 11 benchmarks of node-, link-, and graph-prediction. For example, GATv2 outperforms extensively tuned GNNs by over 1.4% in the difficult “UnseenProj Test” set of the VarMisuse task (Allamanis et al., 2018), without any hyperparameter tuning; and GATv2 improves over an extensively-tuned GAT by 11.5% in 13 prediction objectives in QM9. In node-prediction benchmarks from OGB (Hu et al., 2020), not only that GATv2 outperforms GAT with respect to accuracy – we find that GATv2 is also much more robust to noise.

2 Preliminaries

A directed graph $\mathcal{G} = (\mathcal{V}, \mathcal{E})$ contains nodes $\mathcal{V} = \{1, \dots, n\}$ and edges $\mathcal{E} \subseteq \mathcal{V} \times \mathcal{V}$, where $(j, i) \in \mathcal{E}$ denotes an edge from a node j to a node i . We assume that every node $i \in \mathcal{V}$ has an initial representation $\mathbf{h}_i^{(0)} \in \mathbb{R}^{d_0}$. An undirected graph can be represented with bidirectional edges.

2.1 Graph Neural Networks

A graph neural network (GNN) layer updates every node representation by aggregating its neighbors' representations. A layer's input is a set of node representations $\{\mathbf{h}_i \in \mathbb{R}^d \mid i \in \mathcal{V}\}$ and the set of edges \mathcal{E} . A layer outputs a new set of node representations $\{\mathbf{h}'_i \in \mathbb{R}^{d'} \mid i \in \mathcal{V}\}$, where the same parametric function is applied to every node given its neighbors $\mathcal{N}_i = \{j \in \mathcal{V} \mid (j, i) \in \mathcal{E}\}$:

$$\mathbf{h}'_i = f_\theta(\mathbf{h}_i, \text{AGGREGATE}(\{\mathbf{h}_j \mid j \in \mathcal{N}_i\})) \quad (1)$$

The design of f and `AGGREGATE` is what mostly distinguishes one type of GNN from the other. For example, a common variant of GraphSAGE (Hamilton et al., 2017) performs an element-wise mean as `AGGREGATE`, followed by concatenation with \mathbf{h}_i , a linear layer and a ReLU as f .

2.2 Graph Attention Networks

GraphSAGE and many other popular GNN architectures (Xu et al., 2019; Duvenaud et al., 2015) weigh all neighbors $j \in \mathcal{N}_i$ with *equal importance* (e.g., mean or max-pooling as `AGGREGATE`). To address this limitation, GAT (Veličković et al., 2018) instantiates Equation (1) by computing a learned weighted average of the representations of \mathcal{N}_i . A scoring function $e : \mathbb{R}^d \times \mathbb{R}^d \rightarrow \mathbb{R}$ computes a score for every edge (j, i) , which indicates the importance of the features of the neighbor j to the node i :

$$e(\mathbf{h}_i, \mathbf{h}_j) = \text{LeakyReLU}(\mathbf{a}^\top \cdot [\mathbf{W}\mathbf{h}_i \parallel \mathbf{W}\mathbf{h}_j]) \quad (2)$$

where $\mathbf{a} \in \mathbb{R}^{2d'}$, $\mathbf{W} \in \mathbb{R}^{d' \times d}$ are learned, and \parallel denotes vector concatenation. These attention scores are normalized across all neighbors $j \in \mathcal{N}_i$ using softmax, and the attention function is defined as:

$$\alpha_{ij} = \text{softmax}_j(e(\mathbf{h}_i, \mathbf{h}_j)) = \frac{\exp(e(\mathbf{h}_i, \mathbf{h}_j))}{\sum_{j' \in \mathcal{N}_i} \exp(e(\mathbf{h}_i, \mathbf{h}_{j'}))} \quad (3)$$

Then, GAT computes a weighted average of the transformed features of the neighbor nodes (followed by a nonlinearity σ) as the new representation of i , using the normalized attention coefficients:

$$\mathbf{h}'_i = \sigma\left(\sum_{j \in \mathcal{N}_i} \alpha_{ij} \cdot \mathbf{W}\mathbf{h}_j\right) \quad (4)$$

From now on, we will refer to Equations (2) to (4) as the definition of GAT.

3 The Expressive Power of Graph Attention Mechanisms

In this section, we explain why attention is limited when it is not *dynamic* (Section 3.1). We then show that GAT is severely constrained, because it can only compute *static* attention (Section 3.2). Next, we show how GAT can be fixed (Section 3.3), by simply modifying the order of operations.

We refer to a neural architecture (e.g., the scoring or the attention function of GAT) as a *family of functions*, parameterized by the learned parameters. An element in the family is a concrete function with specific trained weights. In the following, we use $[n]$ to denote the set $[n] = \{1, 2, \dots, n\} \subset \mathbb{N}$.

3.1 The Importance of Dynamic Weighting

Attention is a mechanism for computing a distribution over a set of input *key* vectors, given an additional *query* vector. If the attention function always weighs one key at least as much as any other key, *unconditioned on the query*, we say that this attention function is *static*:

Definition 3.1 (Static attention). A (possibly infinite) family of scoring functions $\mathcal{F} \subseteq (\mathbb{R}^d \times \mathbb{R}^d \rightarrow \mathbb{R})$ computes *static scoring* for a given set of key vectors $\mathbb{K} = \{\mathbf{k}_1, \dots, \mathbf{k}_n\} \subset \mathbb{R}^d$ and query vectors $\mathbb{Q} = \{\mathbf{q}_1, \dots, \mathbf{q}_m\} \subset \mathbb{R}^d$, if for every $f \in \mathcal{F}$ there exists a “highest scoring” key $j_f \in [n]$ such that for every query $i \in [m]$ and key $j \in [n]$ it holds that $f(\mathbf{q}_i, \mathbf{k}_{j_f}) \geq f(\mathbf{q}_i, \mathbf{k}_j)$. We say that a family of attention functions computes *static attention* given \mathbb{K} and \mathbb{Q} , if its scoring function computes static scoring, possibly followed by monotonic normalization such as softmax.

Static attention is very limited because every function $f \in \mathcal{F}$ has a key that is *always selected*, regardless of the query. Such functions cannot model situations where different keys have different relevance to different queries. Static attention is demonstrated in Figure 1a.

The general and powerful form of attention is *dynamic attention*:

Definition 3.2 (Dynamic attention). A (possibly infinite) family of scoring functions $\mathcal{F} \subseteq (\mathbb{R}^d \times \mathbb{R}^d \rightarrow \mathbb{R})$ computes *dynamic scoring* for a set of key vectors $\mathbb{K} = \{\mathbf{k}_1, \dots, \mathbf{k}_n\} \subset \mathbb{R}^d$ and a set of query vectors $\mathbb{Q} = \{\mathbf{q}_1, \dots, \mathbf{q}_m\} \subset \mathbb{R}^d$, if for *any* mapping $\varphi: [m] \rightarrow [n]$ there exists $f \in \mathcal{F}$ such that for any query $i \in [m]$ and any key $j_{\neq \varphi(i)} \in [n]$: $f(\mathbf{q}_i, \mathbf{k}_{\varphi(i)}) > f(\mathbf{q}_i, \mathbf{k}_j)$. We say that a family of attention functions computes *dynamic attention* for \mathbb{K} and \mathbb{Q} , if its scoring function computes dynamic scoring, possibly followed by monotonic normalization such as softmax.

That is, dynamic attention can *select* every key $\varphi(i)$ using the query i , by making $f(\mathbf{q}_i, \mathbf{k}_{\varphi(i)})$ the maximal in $\{f(\mathbf{q}_i, \mathbf{k}_j) \mid j \in [n]\}$. Note that *Dynamic* and *static* attention are exclusive properties, but they are not complementary. Further, every *dynamic* attention family has strict subsets of *static* attention families with respect to the same \mathbb{K} and \mathbb{Q} . Dynamic attention is demonstrated in Figure 1b.

Attending by decaying Another way to think about attention is the ability to “focus” on the most relevant inputs, given a query. Focusing is only possible by *decaying* other inputs, i.e., giving these decayed inputs lower scores than others. If one key is always given an equal or greater attention score than other keys (as in static attention), no query can decay or ignore this key.

3.2 The Limited Expressivity of GAT

Although the scoring function e can be defined in various ways, the original definition of Veličković et al. (2018) (Equation (2)) has become the *de facto* practice: it has spread to a variety of domains (Zhang et al., 2020; Yang et al., 2020; Wang et al., 2019c; Huang and Carley, 2019; Ma et al., 2020; Kosaraju et al., 2019; Nathani et al., 2019; Wu et al., 2020), and is now the standard implementation of “graph attention network” in all popular GNN libraries (Fey and Lenssen, 2019; Wang et al., 2019b; Dwivedi et al., 2020; Gordić, 2020; Brockschmidt, 2020).

The motivation of GAT is to compute a representation for every node as a weighted average of its neighbors. Statedly, GAT is inspired by the attention mechanism of Bahdanau et al. (2014) and the self-attention mechanism of the Transformer (Vaswani et al., 2017). Nonetheless:

Theorem 1. *A GAT layer computes only static attention, for any set of node representations $\mathbb{K} = \mathbb{Q} = \{\mathbf{h}_1, \dots, \mathbf{h}_n\}$. In particular, for $n > 1$, a GAT layer does not compute dynamic attention.*

Proof. Let $\mathcal{G} = (\mathcal{V}, \mathcal{E})$ be a graph modeled by a GAT layer with some \mathbf{a} and \mathbf{W} values (Equations (2) and (3)), and having node representations $\{\mathbf{h}_1, \dots, \mathbf{h}_n\}$. The learned parameter \mathbf{a} can be written as a concatenation $\mathbf{a} = [\mathbf{a}_1 \parallel \mathbf{a}_2] \in \mathbb{R}^{2d'}$ such that $\mathbf{a}_1, \mathbf{a}_2 \in \mathbb{R}^{d'}$, and Equation (2) can be re-written as:

$$e(\mathbf{h}_i, \mathbf{h}_j) = \text{LeakyReLU}(\mathbf{a}_1^\top \mathbf{W} \mathbf{h}_i + \mathbf{a}_2^\top \mathbf{W} \mathbf{h}_j) \quad (5)$$

Since \mathcal{V} is finite, there exists a node $j_{max} \in \mathcal{V}$ such that $\mathbf{a}_2^\top \mathbf{W} \mathbf{h}_{j_{max}}$ is maximal among all nodes $j \in \mathcal{V}$. Due to the monotonicity of LeakyReLU and softmax, for every query node $i \in \mathcal{V}$, the node j_{max} also leads to the maximal value of its attention distribution $\{\alpha_{ij} \mid j \in \mathcal{V}\}$. Thus, α computes only *static attention*. This also implies that α does not compute dynamic attention, because Definition 3.2 holds only for *constant* mappings φ that map all inputs to the same output. \square

The consequence of Theorem 1 is that for any set of nodes \mathcal{V} and a trained GAT layer, the attention function α defines a constant ranking (*argsort*) of the nodes, unconditioned on the query nodes i . That is, we can denote $s_j = \mathbf{a}_2^\top \mathbf{W} \mathbf{h}_j$ and get that for any choice of \mathbf{h}_i , α is monotonic with respect to the per-node scores $\{s_j \mid j \in \mathcal{V}\}$. This global ranking induces the local ranking of every neighborhood \mathcal{N}_i . The only effect of \mathbf{h}_i is in the “sharpness” of the produced attention distribution. This is demonstrated in Figure 1a (bottom), where different curves denote different queries (\mathbf{h}_i).

Generalization to multi-head attention Veličković et al. (2018) found it beneficial to employ H separate attention heads and concatenate their outputs, similarly to Transformers. In this case, Theorem 1 holds for each head separately: every head h has a (possibly different) node that maximizes $\{s_j^{(h)} \mid j \in \mathcal{V}\}$, and the output is the concatenation of H static attention heads.

3.3 Building Dynamic Graph Attention Networks

To create *dynamic* graph attention networks, we modify the order of internal operations in GAT and introduce GATv2 – a simple fix of GAT that is strictly more expressive.

GATv2 The main problem in the standard GAT scoring function (Equation (2)) is that the learned layers \mathbf{W} and \mathbf{a} are applied consecutively, and thus can be collapsed into a single linear layer. To fix this limitation, we simply apply the \mathbf{a} layer after the nonlinearity and the \mathbf{W} layer after the concatenation,¹ effectively applying an MLP to compute the score for each query-key pair:

$$\text{GAT (Veličković et al., 2018):} \quad e(\mathbf{h}_i, \mathbf{h}_j) = \text{LeakyReLU}(\mathbf{a}^\top \cdot [\mathbf{W}\mathbf{h}_i \parallel \mathbf{W}\mathbf{h}_j]) \quad (6)$$

$$\text{GATv2 (our fixed version):} \quad e(\mathbf{h}_i, \mathbf{h}_j) = \mathbf{a}^\top \text{LeakyReLU}(\mathbf{W} \cdot [\mathbf{h}_i \parallel \mathbf{h}_j]) \quad (7)$$

The simple modification makes a significant difference in the expressiveness of the attention function:

Theorem 2. *A GATv2 layer computes dynamic attention for any set of node representations $\mathbb{K} = \mathbb{Q} = \{\mathbf{h}_1, \dots, \mathbf{h}_n\}$.*

We prove Theorem 2 in Appendix A. The main idea is that we can define an appropriate function that GATv2 will be a universal approximator (Cybenko, 1989; Hornik, 1991) of. In contrast, GAT (Equation (52)) cannot approximate any such desired function (Theorem 1).

DPGAT We also consider DPGAT which follows Luong et al. (2015) and the scaled dot-product attention of Vaswani et al. (2017), and is *theoretically weaker* than GATv2. DPGAT is defined as:

$$\text{DPGAT (Vaswani et al., 2017):} \quad e(\mathbf{h}_i, \mathbf{h}_j) = \left((\mathbf{h}_i^\top \mathbf{Q}) \cdot (\mathbf{h}_j^\top \mathbf{K}) \right) / \sqrt{d_k} \quad (8)$$

Variants of DPGAT were used in prior work (Gao and Ji, 2019; Dwivedi and Bresson, 2020; Rong et al., 2020a; Veličković et al., 2020; Kim and Oh, 2021), and we consider it here for the conceptual and empirical comparison with GAT. DPGAT provably performs dynamic attention for any set of node representations that are linearly independent (see Theorem 3 and its proof in Appendix B). Otherwise, there are examples of node representations that *are* linearly dependent and mappings φ , for which dynamic attention does not hold (Appendix B.1). This constraint is not harmful when violated in practice, because every node has only a small set of neighbors, rather than all possible nodes in the graph; further, some nodes possibly never need to be “selected” in practice.

Complexity GATv2 and DPGAT have the same time-complexity as GAT’s declared complexity: $\mathcal{O}(|\mathcal{V}|dd' + |\mathcal{E}|d')$. However, by merging its linear layers, GAT can be computed faster than stated by Veličković et al. (2018). For a detailed time- and parametric-complexity analysis, see Appendix C.

Static vs. dynamic graph problems Many prior GAT-based models had focused on datasets that apparently did not require dynamic attention, where the data had an underlying static ranking of “globally important” nodes. With the growing popularity of GNNs, their adoption expanded to domains that required more complex interactions, and thus required dynamic attention that depends on the representation of the query node as well. In this paper, we revisit the traditional assumptions and show that many modern graph benchmarks and datasets *require dynamic attention* (Section 4).

4 Evaluation

First, we demonstrate the weakness of GAT using a simple synthetic problem that GAT cannot even fit, but is easily solvable by GATv2 (Section 4.1). Second, we show that GATv2 and DPGAT are much more *robust to edge noise*, because their dynamic attention mechanisms allow them to decay noisy (false) edges, while GAT’s performance severely decreases as noise increases (Section 4.2). Finally, we compare GAT, GATv2, and DPGAT across 11 benchmarks overall. (Sections 4.3 to 4.6). We find that GAT is always inferior to GNNs that perform dynamic attention such as GATv2.

Setup All models use skip connections (He et al., 2016) as in Veličković et al. (2018). When previous results exist, we take hyperparameters that were tuned for GAT and use them in GATv2 and DPGAT, without any additional tuning. Self-supervision (Kim and Oh, 2021; Rong et al., 2020a; Hassani and Khasahmadi, 2020), graph regularization methods (Wang et al., 2019a; Zhao and Akoglu, 2020; Rong et al., 2020b), and other tricks (Wang, 2021; Huang et al., 2021) are orthogonal to the contribution of the GNN layer itself, and might further improve all GNNs. In all experiments of GATv2 and DPGAT, we constrain the learned matrix by setting $\mathbf{W} = [\mathbf{W}' \parallel \mathbf{W}']$ in GATv2 and $\mathbf{Q} = \mathbf{K}$ in DPGAT, to rule out the increased number of parameters over GAT as the source of empirical difference (see

¹We also add a bias vector \mathbf{b} before applying the nonlinearity, we omit this in Equation (7) for brevity.

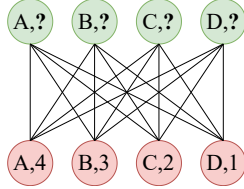


Figure 2: The DICTIONARYLOOKUP problem of size $k=4$: every node in the bottom row has an alphabetic *attribute* ($\{A, B, C, \dots\}$) and a numeric *value* ($\{1, 2, 3, \dots\}$); every node in the upper row has only an attribute; the goal is to predict the value for each node in the upper row, using its attribute.

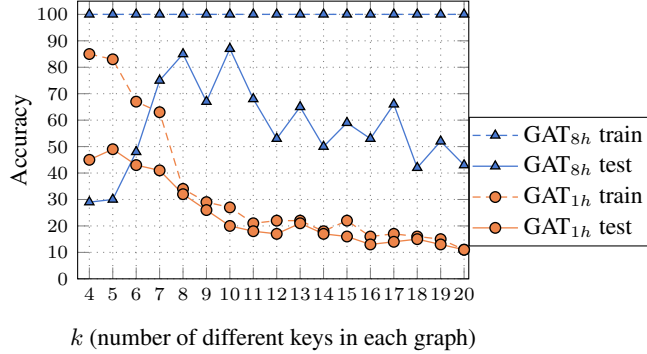


Figure 3: The DICTIONARYLOOKUP problem: GATv2 (not shown) easily achieves 100% train and test accuracy even for $k=100$ and using only a single head.

Appendix C.2). Training details and data statistics are provided in the Appendix E. An implementation of GATv2 is available at https://github.com/tech-srl/how_attentive_are_gats, the rest of the code will be made publicly available.

Our main goal is to compare dynamic and static graph attention mechanisms. However, for reference, we also include non-attentive baselines such as GCN (Kipf and Welling, 2017), GIN (Xu et al., 2019) and GraphSAGE (Hamilton et al., 2017). These non-attentive GNNs can be thought of as a special case of attention, where every node gives all its neighbors the same attention score.

4.1 Synthetic Benchmark: DICTIONARYLOOKUP

The DICTIONARYLOOKUP problem is a contrived problem that we designed to test the ability of a GNN architecture to perform dynamic attention. Here, we demonstrate that GAT cannot learn this simple problem. The graph in Figure 2 is a bipartite graph of $2k$ nodes. Each “key node” in the bottom row has an *attribute* and a *value*. Each “query node” in the upper row has *only an attribute*. The goal is to predict the value of every query node (upper row), according to its attribute. Each graph in the dataset has a different mapping from attributes to values. We created a separate dataset for each $k = \{1, 2, 3, \dots\}$, for which we trained a different model, and measured per-node accuracy.

This problem tests the layer itself because it can be solved using a *single* GNN layer, without suffering from multi-layer side-effects such as over-smoothing (Li et al., 2018; Wu et al., 2020), over-squashing (Alon and Yahav, 2021), or vanishing gradients (Li et al., 2019). Our PyTorch Geometric code will be made publicly available, to serve as a testbed for future graph attention mechanisms.

Results Figure 3 shows the following surprising results: GAT with a single head (GAT_{1h}) failed to fit the training set for any value of k , no matter for how many iterations it was trained, and after trying various training methods (see Appendix D). Thus, it expectedly fails to generalize (resulting in low test accuracy). Using 8 heads, GAT_{8h} successfully fits the *training* set, but generalizes poorly on the *test* set. In contrast, GATv2 and DPGAT easily achieve 100% training and 100% test accuracies, even for $k=100$ (not shown) and using a *single head*, thanks to their ability to perform dynamic attention. These results clearly show the limitations of GAT, which are easily solved by GATv2. An additional comparison to GIN, which could *not* fit this dataset, is provided in Appendix F.1.

The role of multi-head attention Veličković et al. (2018) found the role of multi-head attention to be stabilizing the learning process. Nevertheless, Figure 3 shows that increasing the number of heads has an even more important role – strictly increasing the expressiveness. This is evident by the increased training accuracy of GAT_{8h} over GAT_{1h}, which could not even fit the training set.

Figure 1a (top) shows a heatmap of GAT’s learned attention scores. As shown, all query nodes q_0 to q_9 (the nodes in the upper row of Figure 2) attend mostly to the eighth key (k_8), and have the same ranking of attention coefficients (Figure 1a (bottom)). In contrast, Figure 1b shows how GATv2 can *select* the relevant key node for every query node, because it can compute dynamic attention.

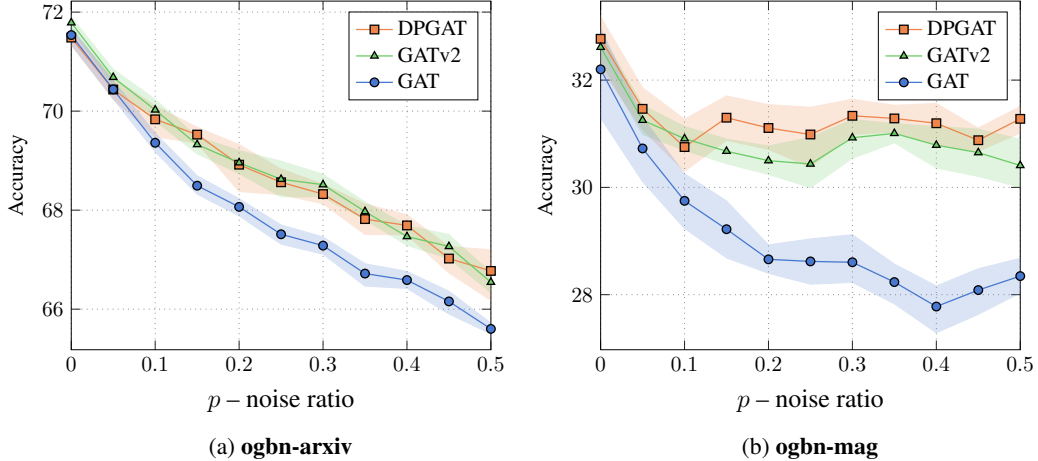


Figure 4: Test accuracy compared to the noise ratio: GATv2 and DPGAT are more robust to structural noise compared to GAT. Each point is an average of 10 runs, error bars show standard deviation.

4.2 Robustness to Noise

We examine the robustness of *dynamic* and *static* attention to noise. In particular, we focus on structural noise: given an input graph $\mathcal{G} = (\mathcal{V}, \mathcal{E})$ and a noise ratio $0 \leq p \leq 1$, we randomly sample $|\mathcal{E}| \times p$ non-existing edges \mathcal{E}' from $\mathcal{V} \times \mathcal{V} \setminus \mathcal{E}$. We then train the GNN on the noisy graph $\mathcal{G}' = (\mathcal{V}, \mathcal{E} \cup \mathcal{E}')$.

Results Figure 4 shows the accuracy on two node-prediction datasets from the Open Graph Benchmark (OGB; Hu et al., 2020) as a function of the noise ratio p . As p increases, all models show a natural decline in test accuracy in both datasets. Yet, thanks to their ability to compute *dynamic* attention, GATv2 and DPGAT show a milder degradation in accuracy compared to GAT, which shows a steeper descent. We hypothesize that the ability to perform *dynamic* attention helps the models distinguishing between given data edges (\mathcal{E}) and noise edges (\mathcal{E}'); in contrast, GAT cannot distinguish between edges, because it scores the source and target nodes separately. These results demonstrate the robustness of *dynamic* attention over *static* attention in such noisy data scenarios.

4.3 Programs: VARMISUSE

Setup VARMISUSE (Allamanis et al., 2018) is an inductive node-pointing problem that depends on 11 types of syntactic and semantic interactions between elements in computer programs. We used the framework of Brockschmidt (2020), who performed an extensive hyperparameter tuning by searching over 30 configurations for every GNN type. We took their best GAT hyperparameters and used them to train GATv2 and DPGAT, without any further tuning.

Results As shown in Table 1, GATv2 and DPGAT are more accurate than GAT and other GNNs in the SeenProj test sets; GATv2 achieves an even higher improvement in the UnseenProj test set. Overall, these results demonstrate the power of GATv2 in modeling complex relational problems, especially since it outperforms extensively tuned models, without any tuning by us.

	Model	SeenProj	UnseenProj
No-Attention	GCN [†]	87.2 \pm 1.5	81.4 \pm 2.3
	GIN [†]	87.1 \pm 0.1	81.1 \pm 0.9
Attention	GAT [†]	86.9 \pm 0.7	81.2 \pm 0.9
	DPGAT	88.0 \pm 0.8	81.5 \pm 1.2
	GATv2	88.0 \pm 1.1	82.8 \pm 1.7

Table 1: Accuracy (5 runs \pm stdev) on VARMISUSE. GATv2 is more accurate than all GNNs in both test sets, using GAT’s hyperparameters. [†] – previously reported by Brockschmidt (2020).

4.4 Node-Prediction

We further compare GATv2, GAT, and other GNNs on four node-prediction datasets from OGB.

	Model	ogbn-arxiv	ogbn-products	ogbn-mag	ogbn-proteins
No-Attention	GCN [†]	71.74±0.29	78.97±0.33	30.43±0.25	72.51±0.35
	GraphSAGE [†]	71.49±0.27	78.70±0.36	31.53±0.15	77.68±0.20
Attention 1 head	GAT _{1h}	71.59±0.38	79.04±1.54	32.20±1.46	70.77±5.79
	DPGAT _{1h}	71.52±0.17	76.49±0.78	32.77 ±0.80	63.47±2.79
	GATv2 _{1h}	71.78±0.18	80.63 ±0.70	32.61±0.44	77.23±3.32
Attention 8 heads	GAT _{8h}	71.54±0.30	77.23±2.37	31.75±1.60	78.63±1.62
	DPGAT _{8h}	71.48±0.26	73.53±0.47	27.74±9.97	72.88±0.59
	GATv2 _{8h}	71.87 ±0.25	78.46±2.45	32.52±0.39	79.52 ±0.55

(a)

(b)

Table 2: Average accuracy (Table 2a) and ROC-AUC (Table 2b) in node-prediction datasets (10 runs±std). In all datasets, GATv2 outperforms GAT. † – previously reported by Hu et al. (2020).

	Model	ogbl-collab		ogbl-citation2
		w/o val edges	w/ val edges	
No-Attention	GCN [†]	44.75±1.07	47.14±1.45	80.04±0.25
	GraphSAGE [†]	48.10±0.81	54.63±1.12	80.44 ±0.10
Attention 1 head	GAT _{1h}	39.32±3.26	48.10±4.80	79.84±0.19
	DPGAT _{1h}	44.15±1.59	49.61±3.16	80.31±0.21
	GATv2 _{1h}	42.00±2.40	48.02±2.77	80.33±0.13
Attention 8 heads	GAT _{8h}	42.37±2.99	46.63±2.80	75.95±1.31
	DPGAT _{8h}	48.99 ±0.70	56.90 ±1.45	79.64±0.42
	GATv2 _{8h}	42.85±2.64	49.70±3.08	80.14±0.71

(a)

(b)

Table 3: Average Hits@50 (Table 3a) and mean reciprocal rank (MRR) (Table 3b) in link-prediction benchmarks from OGB (10 runs±std). † – previously reported by Hu et al. (2020).

Results Results are shown in Table 2. In all settings and all datasets, GATv2 is more accurate than GAT and the non-attentive GNNs, and GATv2 is more accurate than DPGAT in all settings except one. Interestingly, in the datasets of Table 2a, there is no significant difference between using 1 or 8 heads; however in Table 2b (**ogbn-proteins**), increasing the number of heads results in a major improvement for GAT, while GATv2 already gets most of the benefit using a single attention head. These results demonstrate the superiority of GATv2 over GAT, thanks to GATv2’s dynamic attention.

4.5 Link-Prediction

We compare GATv2, GAT, and other GNNs in link-prediction datasets from OGB.

Results Results are shown in Table 3. In **ogbl-collab** (Table 3a), DPGAT_{8h} achieves higher accuracy than all models. This is consistent with Kim and Oh (2021), who found that DPGAT predicts edge presence better, but in much smaller datasets (Cora, CiteSeer, PubMed, and PPI). In **ogbl-citation2** (Table 3b), GATv2 achieves a higher MRR than GAT and DPGAT with the same number of heads, but the non-attentive GraphSAGE performs better than all attentive GNNs. We hypothesize that attention is not needed in this dataset. In all datasets, the lowest score is achieved by a standard GAT.

4.6 Graph-Prediction: QM9

Setup In the QM9 dataset (Ramakrishnan et al., 2014; Gilmer et al., 2017) contains ~130,000 graphs with ~18 nodes. Each graph is a molecule where nodes are atoms, and the goal is to regress each graph to 13 real-valued quantum chemical properties. We used the implementation of Brockschmidt (2020) who performed an extensive hyperparameter search over 500 configurations; we took their best-found configurations and modified the code of GAT to implement GATv2 and DPGAT.

Model	Predicted Property													Rel. to GAT _{8h}
	1	2	3	4	5	6	7	8	9	10	11	12	13	
GCN [†]	3.21	4.22	1.45	1.62	2.42	16.38	17.40	7.82	8.24	9.05	7.00	3.93	1.02	-1.5%
GIN [†]	2.64	4.67	1.42	1.50	2.27	15.63	12.93	5.88	18.71	5.62	5.38	3.53	1.05	-2.3%
GAT _{1h}	3.08	7.82	1.79	3.96	3.58	35.43	116.5	28.10	20.80	15.80	10.80	5.37	3.11	+134.1%
DPGAT _{1h}	3.20	8.35	1.71	2.17	2.88	25.21	65.79	12.93	13.32	14.42	13.83	6.37	3.28	+77.9%
GATv2 _{1h}	3.04	6.38	1.68	2.18	2.82	20.56	77.13	10.19	22.56	15.04	22.94	5.23	2.46	+91.6%
GAT _{8h} [†]	2.68	4.65	1.48	1.53	2.31	52.39	14.87	7.61	6.86	7.64	6.54	4.11	1.48	+0%
DPGAT _{8h}	2.63	4.37	1.44	1.40	2.10	32.59	11.66	6.95	7.09	7.30	6.52	3.76	1.18	-9.7%
GATv2 _{8h}	2.65	4.28	1.41	1.47	2.29	16.37	14.03	6.07	6.28	6.60	5.97	3.57	1.59	-11.5%

Table 4: Average error rates (lower is better), 5 runs for each property, on the QM9 dataset. † was previously tuned and reported by Brockschmidt (2020). Standard deviation is reported in Appendix F.

Results Results are shown in Table 4. The main results are that GATv2 achieves a lower (better) error rate than GAT, with both 8 and a single attention head. Overall, GATv2 achieves the lowest average error rate. GAT_{1h} achieves the overall highest error rate, and GAT_{8h} achieves the highest error rate among the attentive GNNs that use 8 heads and among the non-attentive GNNs.

5 Related Work

Attention in GNNs Modeling pairwise interactions between elements in graph-structured data goes back to interaction networks (Battaglia et al., 2016; Hoshen, 2017) and relational networks (Santoro et al., 2017). The GAT formulation of Veličković et al. (2018) rose as the most popular framework for attentional GNNs, thanks to its simplicity, generality, and applicability beyond reinforcement learning (Denil et al., 2017; Duan et al., 2017). Nevertheless, in this work, we show that the popular and widespread definition of GAT is severely constrained to static attention only.

Transformers and GNNs Many works employed GNNs with Transformer-style attention (dot-product) (Zhang et al., 2018; Thekumparampil et al., 2018; Gao and Ji, 2019; Lukovnikov and Fischer, 2021; Shi et al., 2020; Dwivedi and Bresson, 2020; Busbridge et al., 2019; Rong et al., 2020a; Veličković et al., 2020), and Lee et al. (2018) conducted an extensive survey of attention types in GNNs. However, none of these works identified the monotonicity of GAT’s attention mechanism, the theoretical differences between attention types, nor empirically compared their performance. Kim and Oh (2021) compared the standard GAT with dot-product attention empirically, but in a specific self-supervised scenario, without observing the theoretical difference in their expressiveness.

The static attention of GAT Qiu et al. (2018) recognized the order-preserving property of GAT, but did not identify the severe theoretical constraint that this property implies: the inability to perform dynamic attention (Theorem 1). Furthermore, they presented GAT’s monotonicity as a *desired* trait (!) To the best of our knowledge, our work is the first work to recognize the inability of GAT to perform dynamic attention and its practical harmful consequences.

6 Conclusion

In this paper, we identify that the popular and widespread Graph Attention Networks do not compute *dynamic* attention. Instead, the attention mechanism in the standard definition and implementations of GAT is only *static*, and for any query, its scoring is monotonic with respect to per-node scores. As a result, GAT cannot even express simple alignment problems. To address this limitation, we introduce a simple fix and propose GATv2: by modifying the order of operations in GAT, GATv2 achieves a universal approximator attention function and is thus strictly more powerful than GAT.

We demonstrate the empirical advantage of GATv2 over GAT in a controlled problem that requires alignment of nodes, and in 11 OGB and additional public benchmarks overall. Our experiments show that GATv2 outperforms GAT in all benchmarks while having the same parametric cost.

We encourage the community to use GATv2 instead of GAT whenever comparing new GNN architectures to the common strong baselines. In complex tasks and domains, a model that uses GAT as an internal component can replace it with GATv2 to benefit from a strictly more powerful model. To this end, we will make our code publicly available at https://github.com/tech-srl/how_attentive_are_gats.

Acknowledgments

We thank Gail Weiss for the helpful discussions, thorough feedback, and inspirational paper (Weiss et al., 2018). We also thank Petar Veličković for the useful discussion about the complexity and implementation of GAT.

References

- Miltiadis Allamanis, Marc Brockschmidt, and Mahmoud Khademi. Learning to represent programs with graphs. In *International Conference on Learning Representations*, 2018. URL <https://openreview.net/forum?id=BJOFETxR->.
- Uri Alon and Eran Yahav. On the bottleneck of graph neural networks and its practical implications. In *International Conference on Learning Representations*, 2021. URL <https://openreview.net/forum?id=i800Ph0CVH2>.
- James Atwood and Don Towsley. Diffusion-convolutional neural networks. In *Advances in neural information processing systems*, pages 1993–2001, 2016.
- Dzmitry Bahdanau, Kyunghyun Cho, and Yoshua Bengio. Neural machine translation by jointly learning to align and translate. *CoRR*, abs/1409.0473, 2014. URL <http://arxiv.org/abs/1409.0473>.
- Peter Battaglia, Razvan Pascanu, Matthew Lai, Danilo Jimenez Rezende, and Koray kavukcuoglu. Interaction networks for learning about objects, relations and physics. In *Proceedings of the 30th International Conference on Neural Information Processing Systems*, pages 4509–4517, 2016.
- Marc Brockschmidt. Gnn-film: Graph neural networks with feature-wise linear modulation. *Proceedings of the 36th International Conference on Machine Learning, ICML*, 2020.
- Michael M Bronstein, Joan Bruna, Yann LeCun, Arthur Szlam, and Pierre Vandergheynst. Geometric deep learning: going beyond euclidean data. *IEEE Signal Processing Magazine*, 34(4):18–42, 2017.
- Michael M. Bronstein, Joan Bruna, Taco Cohen, and Petar Veličković. Geometric deep learning: Grids, groups, graphs, geodesics, and gauges, 2021.
- Dan Busbridge, Dane Sherburn, Pietro Cavallo, and Nils Y Hammerla. Relational graph attention networks. *arXiv preprint arXiv:1904.05811*, 2019.
- George Cybenko. Approximation by superpositions of a sigmoidal function. *Mathematics of control, signals and systems*, 2(4):303–314, 1989.
- Misha Denil, Sergio Gómez Colmenarejo, Serkan Cabi, David Saxton, and Nando de Freitas. Programmable agents. *arXiv preprint arXiv:1706.06383*, 2017.
- Yan Duan, Marcin Andrychowicz, Bradly Stadie, Jonathan Ho, Jonas Schneider, Ilya Sutskever, Pieter Abbeel, and Wojciech Zaremba. One-shot imitation learning. In *Proceedings of the 31st International Conference on Neural Information Processing Systems*, pages 1087–1098, 2017.
- David K Duvenaud, Dougal Maclaurin, Jorge Iparraguirre, Rafael Bombarell, Timothy Hirzel, Alán Aspuru-Guzik, and Ryan P Adams. Convolutional networks on graphs for learning molecular fingerprints. In *Advances in neural information processing systems*, pages 2224–2232, 2015.
- Vijay Prakash Dwivedi and Xavier Bresson. A generalization of transformer networks to graphs. *arXiv preprint arXiv:2012.09699*, 2020.
- Vijay Prakash Dwivedi, Chaitanya K Joshi, Thomas Laurent, Yoshua Bengio, and Xavier Bresson. Benchmarking graph neural networks. *arXiv preprint arXiv:2003.00982*, 2020.
- Matthias Fey and Jan E. Lenssen. Fast graph representation learning with PyTorch Geometric. In *ICLR Workshop on Representation Learning on Graphs and Manifolds*, 2019.

- Ken-Ichi Funahashi. On the approximate realization of continuous mappings by neural networks. *Neural networks*, 2(3):183–192, 1989.
- Hongyang Gao and Shuiwang Ji. Graph representation learning via hard and channel-wise attention networks. In *Proceedings of the 25th ACM SIGKDD International Conference on Knowledge Discovery & Data Mining*, pages 741–749, 2019.
- Justin Gilmer, Samuel S Schoenholz, Patrick F Riley, Oriol Vinyals, and George E Dahl. Neural message passing for quantum chemistry. In *Proceedings of the 34th International Conference on Machine Learning-Volume 70*, pages 1263–1272. JMLR. org, 2017.
- Aleksa Gordić. pytorch-gat. <https://github.com/gordicaleksa/pytorch-GAT>, 2020.
- Marco Gori, Gabriele Monfardini, and Franco Scarselli. A new model for learning in graph domains. In *Proceedings. 2005 IEEE International Joint Conference on Neural Networks, 2005.*, volume 2, pages 729–734. IEEE, 2005.
- Will Hamilton, Zitao Ying, and Jure Leskovec. Inductive representation learning on large graphs. In *Advances in neural information processing systems*, pages 1024–1034, 2017.
- Kaveh Hassani and Amir Hosein Khasahmadi. Contrastive multi-view representation learning on graphs. In *International Conference on Machine Learning*, pages 4116–4126. PMLR, 2020.
- Kaiming He, Xiangyu Zhang, Shaoqing Ren, and Jian Sun. Deep residual learning for image recognition. In *Proceedings of the IEEE conference on computer vision and pattern recognition*, pages 770–778, 2016.
- Kurt Hornik. Approximation capabilities of multilayer feedforward networks. *Neural networks*, 4(2):251–257, 1991.
- Kurt Hornik, Maxwell Stinchcombe, and Halbert White. Multilayer feedforward networks are universal approximators. *Neural networks*, 2(5):359–366, 1989.
- Yedid Hoshen. Vain: attentional multi-agent predictive modeling. In *Proceedings of the 31st International Conference on Neural Information Processing Systems*, pages 2698–2708, 2017.
- Weihua Hu, Matthias Fey, Marinka Zitnik, Yuxiao Dong, Hongyu Ren, Bowen Liu, Michele Catasta, and Jure Leskovec. Open graph benchmark: Datasets for machine learning on graphs. *arXiv preprint arXiv:2005.00687*, 2020.
- Binxuan Huang and Kathleen M Carley. Syntax-aware aspect level sentiment classification with graph attention networks. In *Proceedings of the 2019 Conference on Empirical Methods in Natural Language Processing and the 9th International Joint Conference on Natural Language Processing (EMNLP-IJCNLP)*, pages 5472–5480, 2019.
- Qian Huang, Horace He, Abhay Singh, Ser-Nam Lim, and Austin Benson. Combining label propagation and simple models out-performs graph neural networks. In *International Conference on Learning Representations*, 2021. URL <https://openreview.net/forum?id=8E1-f3VhX1o>.
- Chaitanya Joshi. Transformers are graph neural networks. *The Gradient*, 2020.
- Dongkwan Kim and Alice Oh. How to find your friendly neighborhood: Graph attention design with self-supervision. In *International Conference on Learning Representations*, 2021. URL <https://openreview.net/forum?id=Wi5KUNlqWty>.
- Thomas N Kipf and Max Welling. Semi-supervised classification with graph convolutional networks. In *ICLR*, 2017.
- Vineet Kosaraju, Amir Sadeghian, Roberto Martín-Martín, Ian Reid, Hamid Rezaatofighi, and Silvio Savarese. Social-bigat: Multimodal trajectory forecasting using bicycle-gan and graph attention networks. In H. Wallach, H. Larochelle, A. Beygelzimer, F. d Alché-Buc, E. Fox, and R. Garnett, editors, *Advances in Neural Information Processing Systems*, volume 32. Curran Associates, Inc., 2019. URL <https://proceedings.neurips.cc/paper/2019/file/d09bf41544a3365a46c9077ebb5e35c3-Paper.pdf>.
- John Boaz Lee, Ryan A Rossi, Sungchul Kim, Nesreen K Ahmed, and Eunye Koh. Attention models in graphs: A survey. *arXiv preprint arXiv:1807.07984*, 2018.
- Moshe Leshno, Vladimir Ya Lin, Allan Pinkus, and Shimon Schocken. Multilayer feedforward networks with a nonpolynomial activation function can approximate any function. *Neural networks*, 6(6):861–867, 1993.

- Guohao Li, Matthias Muller, Ali Thabet, and Bernard Ghanem. Deepgcns: Can gcns go as deep as cnns? In *Proceedings of the IEEE/CVF International Conference on Computer Vision*, pages 9267–9276, 2019.
- Qimai Li, Zhichao Han, and Xiao-Ming Wu. Deeper insights into graph convolutional networks for semi-supervised learning. In *Thirty-Second AAAI Conference on Artificial Intelligence*, 2018.
- Yujia Li, Daniel Tarlow, Marc Brockschmidt, and Richard Zemel. Gated graph sequence neural networks. In *International Conference on Learning Representations*, 2016.
- Denis Lukovnikov and Asja Fischer. Gated relational graph attention networks, 2021. URL https://openreview.net/forum?id=v-9E8egy_i.
- Thang Luong, Hieu Pham, and Christopher D. Manning. Effective approaches to attention-based neural machine translation. In *Proceedings of the 2015 Conference on Empirical Methods in Natural Language Processing, EMNLP 2015, Lisbon, Portugal, September 17-21, 2015*, pages 1412–1421, 2015. URL <http://aclweb.org/anthology/D/D15/D15-1166.pdf>.
- Nianzu Ma, Sahisnu Mazumder, Hao Wang, and Bing Liu. Entity-aware dependency-based deep graph attention network for comparative preference classification. In *Proceedings of the 58th Annual Meeting of the Association for Computational Linguistics*, pages 5782–5788, 2020.
- Federico Monti, Davide Boscaini, Jonathan Masci, Emanuele Rodola, Jan Svoboda, and Michael M Bronstein. Geometric deep learning on graphs and manifolds using mixture model cnns. In *Proceedings of the IEEE conference on computer vision and pattern recognition*, pages 5115–5124, 2017.
- Deepak Nathani, Jatin Chauhan, Charu Sharma, and Manohar Kaul. Learning attention-based embeddings for relation prediction in knowledge graphs. In *Proceedings of the 57th Annual Meeting of the Association for Computational Linguistics*, pages 4710–4723, 2019.
- Sejun Park, Chulhee Yun, Jaeho Lee, and Jinwoo Shin. Minimum width for universal approximation. In *International Conference on Learning Representations*, 2021. URL <https://openreview.net/forum?id=0-XJwyoIF-k>.
- Allan Pinkus. Approximation theory of the mlp model. *Acta Numerica 1999: Volume 8*, 8:143–195, 1999.
- Jiezhong Qiu, Jian Tang, Hao Ma, Yuxiao Dong, Kuansan Wang, and Jie Tang. Deepinf: Social influence prediction with deep learning. In *Proceedings of the 24th ACM SIGKDD International Conference on Knowledge Discovery and Data Mining (KDD '18)*, 2018.
- Raghunathan Ramakrishnan, Pavlo O Dral, Matthias Rupp, and O Anatole Von Lilienfeld. Quantum chemistry structures and properties of 134 kilo molecules. *Scientific data*, 1:140022, 2014.
- Yu Rong, Yatao Bian, Tingyang Xu, Weiyang Xie, Ying Wei, Wenbing Huang, and Junzhou Huang. Self-supervised graph transformer on large-scale molecular data. *Advances in Neural Information Processing Systems*, 33, 2020a.
- Yu Rong, Wenbing Huang, Tingyang Xu, and Junzhou Huang. Dropedge: Towards deep graph convolutional networks on node classification. In *International Conference on Learning Representations*, 2020b. URL <https://openreview.net/forum?id=Hkx1qkrKPr>.
- Adam Santoro, David Raposo, David GT Barrett, Mateusz Malinowski, Razvan Pascanu, Peter Battaglia, and Timothy Lillicrap. A simple neural network module for relational reasoning. In *Proceedings of the 31st International Conference on Neural Information Processing Systems*, pages 4974–4983, 2017.
- Franco Scarselli, Marco Gori, Ah Chung Tsoi, Markus Hagenbuchner, and Gabriele Monfardini. The graph neural network model. *IEEE Transactions on Neural Networks*, 20(1):61–80, 2008.
- Yunsheng Shi, Zhengjie Huang, Shikun Feng, and Yu Sun. Masked label prediction: Unified message passing model for semi-supervised classification. *arXiv preprint arXiv:2009.03509*, 2020.
- Kiran K Thekumparampil, Chong Wang, Sewoong Oh, and Li-Jia Li. Attention-based graph neural network for semi-supervised learning. *arXiv preprint arXiv:1803.03735*, 2018.
- Ashish Vaswani, Noam Shazeer, Niki Parmar, Jakob Uszkoreit, Llion Jones, Aidan N Gomez, Łukasz Kaiser, and Illia Polosukhin. Attention is all you need. In *Advances in Neural Information Processing Systems*, pages 6000–6010, 2017.
- Petar Veličković, Guillem Cucurull, Arantxa Casanova, Adriana Romero, Pietro Liò, and Yoshua Bengio. Graph attention networks. In *International Conference on Learning Representations*, 2018.

- Petar Veličković, Lars Buesing, Matthew Overlan, Razvan Pascanu, Oriol Vinyals, and Charles Blundell. Pointer graph networks. *Advances in Neural Information Processing Systems*, 33, 2020.
- Guangtao Wang, Rex Ying, Jing Huang, and Jure Leskovec. Improving graph attention networks with large margin-based constraints. *arXiv preprint arXiv:1910.11945*, 2019a.
- Minjie Wang, Da Zheng, Zihao Ye, Quan Gan, Mufei Li, Xiang Song, Jinjing Zhou, Chao Ma, Lingfan Yu, Yu Gai, Tianjun Xiao, Tong He, George Karypis, Jinyang Li, and Zheng Zhang. Deep graph library: A graph-centric, highly-performant package for graph neural networks. *arXiv preprint arXiv:1909.01315*, 2019b.
- Xiao Wang, Houye Ji, Chuan Shi, Bai Wang, Yanfang Ye, Peng Cui, and Philip S Yu. Heterogeneous graph attention network. In *The World Wide Web Conference*, pages 2022–2032, 2019c.
- Yangkun Wang. Bag of tricks of semi-supervised classification with graph neural networks. *arXiv preprint arXiv:2103.13355*, 2021.
- Gail Weiss, Yoav Goldberg, and Eran Yahav. On the practical computational power of finite precision rnns for language recognition. In *Proceedings of the 56th Annual Meeting of the Association for Computational Linguistics (Volume 2: Short Papers)*, pages 740–745, 2018.
- Felix Wu, Amauri Souza, Tianyi Zhang, Christopher Fifty, Tao Yu, and Kilian Weinberger. Simplifying graph convolutional networks. In *International conference on machine learning*, pages 6861–6871. PMLR, 2019.
- Zonghan Wu, Shirui Pan, Fengwen Chen, Guodong Long, Chengqi Zhang, and S Yu Philip. A comprehensive survey on graph neural networks. *IEEE Transactions on Neural Networks and Learning Systems*, 2020.
- Keyulu Xu, Weihua Hu, Jure Leskovec, and Stefanie Jegelka. How powerful are graph neural networks? In *International Conference on Learning Representations*, 2019. URL <https://openreview.net/forum?id=ryGs6iA5Km>.
- Yiding Yang, Jiayan Qiu, Mingli Song, Dacheng Tao, and Xinchao Wang. Distilling knowledge from graph convolutional networks. In *Proceedings of the IEEE/CVF Conference on Computer Vision and Pattern Recognition (CVPR)*, June 2020.
- Hanqing Zeng, Hongkuan Zhou, Ajitesh Srivastava, Rajgopal Kannan, and Viktor Prasanna. Graphsaint: Graph sampling based inductive learning method. *arXiv preprint arXiv:1907.04931*, 2019.
- Jiani Zhang, Xingjian Shi, Junyuan Xie, Hao Ma, Irwin King, and Dit-Yan Yeung. Gaan: Gated attention networks for learning on large and spatiotemporal graphs. In *Proceedings of the Thirty-Fourth Conference on Uncertainty in Artificial Intelligence*, pages 339–349, 2018.
- Kai Zhang, Yaokang Zhu, Jun Wang, and Jie Zhang. Adaptive structural fingerprints for graph attention networks. In *International Conference on Learning Representations*, 2020. URL <https://openreview.net/forum?id=BJxWx0NYPr>.
- Lingxiao Zhao and Leman Akoglu. Pairnorm: Tackling oversmoothing in gnns. In *International Conference on Learning Representations*, 2020. URL <https://openreview.net/forum?id=rkecl1rtwB>.

A Proof for Theorem 2

For brevity, we repeat our definition of dynamic attention (Definition 3.2):

Definition 3.2 (Dynamic attention). A (possibly infinite) family of scoring functions $\mathcal{F} \subseteq (\mathbb{R}^d \times \mathbb{R}^d \rightarrow \mathbb{R})$ computes *dynamic scoring* for a set of key vectors $\mathbb{K} = \{\mathbf{k}_1, \dots, \mathbf{k}_n\} \subset \mathbb{R}^d$ and a set of query vectors $\mathbb{Q} = \{\mathbf{q}_1, \dots, \mathbf{q}_m\} \subset \mathbb{R}^d$, if for *any* mapping $\varphi: [m] \rightarrow [n]$ there exists $f \in \mathcal{F}$ such that for any query $i \in [m]$ and any key $j \neq \varphi(i) \in [n]$: $f(\mathbf{q}_i, \mathbf{k}_{\varphi(i)}) > f(\mathbf{q}_i, \mathbf{k}_j)$. We say that a family of attention functions computes *dynamic attention* for \mathbb{K} and \mathbb{Q} , if its scoring function computes dynamic scoring, possibly followed by monotonic normalization such as softmax.

Theorem 2. A GATv2 layer computes dynamic attention for any set of node representations $\mathbb{K} = \mathbb{Q} = \{\mathbf{h}_1, \dots, \mathbf{h}_n\}$.

Proof. Let $\mathcal{G} = (\mathcal{V}, \mathcal{E})$ be a graph modeled by a GATv2 layer, having node representations $\{\mathbf{h}_1, \dots, \mathbf{h}_n\}$, and let $\varphi: [n] \rightarrow [n]$ be any node mapping $[n] \rightarrow [n]$. We define $g: \mathbb{R}^{2d} \rightarrow \mathbb{R}$ as follows:

$$g(\mathbf{x}) = \begin{cases} 1 & \exists i: \mathbf{x} = [\mathbf{h}_i \| \mathbf{h}_{\varphi(i)}] \\ 0 & \text{otherwise} \end{cases} \quad (9)$$

Next, we define the *continues* function $\tilde{g}: \mathbb{R}^{2d} \rightarrow \mathbb{R}$ that equals to g in specific n^2 inputs:

$$\tilde{g}([\mathbf{h}_i \| \mathbf{h}_j]) = g([\mathbf{h}_i \| \mathbf{h}_j]), \forall i, j \in [n] \quad (10)$$

For all other inputs $x \in \mathbb{R}^{2d}$, $\tilde{g}(x)$ realizes to values that maintain the continuity of \tilde{g} (this is possible because we fixed the values of \tilde{g} for only a finite set of points).

Thus, for every node $i \in \mathcal{V}$ and $j \neq \varphi(i) \in \mathcal{V}$:

$$1 = \tilde{g}([\mathbf{h}_i \| \mathbf{h}_{\varphi(i)}]) > \tilde{g}([\mathbf{h}_i \| \mathbf{h}_j]) = 0 \quad (11)$$

If we concatenate the two input vectors, and define the scoring function e of GATv2 (Equation (7)) as a function of the concatenated vector $[\mathbf{h}_i \| \mathbf{h}_j]$, from the universal approximation theorem (Hornik et al., 1989; Cybenko, 1989; Funahashi, 1989; Hornik, 1991), e can approximate \tilde{g} for any compact subset of \mathbb{R}^{2d} .

Thus, for any sufficiently small ϵ (any $0 < \epsilon < 1/2$) there exist parameters \mathbf{W} and \mathbf{a} such that for every node $i \in \mathcal{V}$ and every $j \neq \varphi(i)$:

$$e_{\mathbf{W}, \mathbf{a}}(\mathbf{h}_i, \mathbf{h}_{\varphi(i)}) > 1 - \epsilon > 0 + \epsilon > e_{\mathbf{W}, \mathbf{a}}(\mathbf{h}_i, \mathbf{h}_j) \quad (12)$$

and due to the increasing monotonicity of softmax:

$$\alpha_{i, \varphi(i)} > \alpha_{i, j} \quad (13)$$

□

The choice of nonlinearity In general, these results hold if GATv2 had used any common non-polynomial activation function (such as ReLU, sigmoid, or the hyperbolic tangent function). The LeakyReLU activation function of GATv2 does not change its universal approximation ability (Leshno et al., 1993; Pinkus, 1999; Park et al., 2021), and it was chosen only for consistency with the original definition of GAT.

B Proof that DPGAT Performs Dynamic Attention

Theorem 3. A DPGAT layer computes dynamic attention for any set of node representations $\mathbb{K} = \mathbb{Q} = \{\mathbf{h}_1, \dots, \mathbf{h}_n\}$ that are linearly independent.

Proof. Let $\mathcal{G} = (\mathcal{V}, \mathcal{E})$ be a graph modeled by a DPGAT layer, having linearly independent node representations $\{\mathbf{h}_1, \dots, \mathbf{h}_n\}$. Let $\varphi: [n] \rightarrow [n]$ be any node mapping $[n] \rightarrow [n]$.

We denote the i^{th} row of a matrix M as M_i .

We define a matrix P as:

$$P_{i,j} = \begin{cases} 1 & j = \varphi(i) \\ 0 & \text{otherwise} \end{cases} \quad (14)$$

Let $\mathbf{X} \in \mathbb{R}^n \times \mathbb{R}^d$ be the matrix holding the graph's node representations as its rows:

$$\mathbf{X} = \begin{bmatrix} - & \mathbf{h}_1 & - \\ - & \mathbf{h}_2 & - \\ & \vdots & \\ - & \mathbf{h}_n & - \end{bmatrix} \quad (15)$$

Since the rows of \mathbf{X} are linearly independent, it necessarily holds that $d \geq n$.

Next, we find weight matrices $\mathbf{Q} \in \mathbb{R}^d \times \mathbb{R}^d$ and $\mathbf{K} \in \mathbb{R}^d \times \mathbb{R}^d$ such that:

$$(\mathbf{XQ}) \cdot (\mathbf{XK})^\top = \mathbf{P} \quad (16)$$

To satisfy Equation (16), we choose \mathbf{Q} and \mathbf{K} such that $\mathbf{XQ} = \mathbf{U}$ and $\mathbf{XK} = \mathbf{P}^\top \mathbf{U}$ where \mathbf{U} is an orthonormal matrix ($\mathbf{U} \cdot \mathbf{U}^\top = \mathbf{U}^\top \cdot \mathbf{U} = \mathbf{I}$).

We can obtain \mathbf{U} using the singular value decomposition (SVD) of \mathbf{X} :

$$\mathbf{X} = \mathbf{U}\mathbf{\Sigma}\mathbf{V}^\top \quad (17)$$

Since $\mathbf{\Sigma} \in \mathbb{R}^n \times \mathbb{R}^n$ and \mathbf{X} has a full rank, $\mathbf{\Sigma}$ is invertible, and thus:

$$\mathbf{XV}\mathbf{\Sigma}^{-1} = \mathbf{U} \quad (18)$$

Now, we define \mathbf{Q} as follows:

$$\mathbf{Q} = \mathbf{V}\mathbf{\Sigma}^{-1} \quad (19)$$

Note that $\mathbf{XQ} = \mathbf{U}$, as desired.

To find \mathbf{K} that satisfies $\mathbf{XK} = \mathbf{P}^\top \mathbf{U}$, we use Equation (17) and require:

$$\mathbf{U}\mathbf{\Sigma}\mathbf{V}^\top \mathbf{K} = \mathbf{P}^\top \mathbf{U} \quad (20)$$

and thus:

$$\mathbf{K} = \mathbf{V}\mathbf{\Sigma}^{-1}\mathbf{U}^\top \mathbf{P}^\top \mathbf{U} \quad (21)$$

We define:

$$z(\mathbf{h}_i, \mathbf{h}_j) = e(\mathbf{h}_i, \mathbf{h}_j) \cdot \sqrt{d_k} \quad (22)$$

Where e is the attention score function of DPGAT (Equation (8)).

Now, for a query i and a key j , and the corresponding representations $\mathbf{h}_i, \mathbf{h}_j$:

$$z(\mathbf{h}_i, \mathbf{h}_j) = (\mathbf{h}_i^\top \mathbf{Q}) \cdot (\mathbf{h}_j^\top \mathbf{K})^\top \quad (23)$$

$$= (\mathbf{X}_i \mathbf{Q}) \cdot (\mathbf{X}_j \mathbf{K})^\top \quad (24)$$

Since $\mathbf{X}_i \mathbf{Q} = (\mathbf{XQ})_i$ and $\mathbf{X}_j \mathbf{K} = (\mathbf{XK})_j$, we get

$$z(\mathbf{h}_i, \mathbf{h}_j) = (\mathbf{XQ})_i \cdot \left((\mathbf{XK})_j \right)^\top = P_{i,j} \quad (25)$$

Therefore:

$$z(\mathbf{h}_i, \mathbf{h}_j) = \begin{cases} 1 & j = \varphi(i) \\ 0 & \text{otherwise} \end{cases} \quad (26)$$

And thus:

$$e(\mathbf{h}_i, \mathbf{h}_j) = \begin{cases} 1/\sqrt{d_k} & j = \varphi(i) \\ 0 & \text{otherwise} \end{cases} \quad (27)$$

To conclude, for every selected query i and any key $j \neq \varphi(i)$:

$$e(\mathbf{h}_i, \mathbf{h}_{\varphi(i)}) > e(\mathbf{h}_i, \mathbf{h}_j) \quad (28)$$

and due to the increasing monotonicity of softmax:

$$\alpha_{i, \varphi(i)} > \alpha_{i, j} \quad (29)$$

Hence, a DPGAT layer computes dynamic attention.

In the case that $d > n$, we apply SVD to the full-rank matrix $\mathbf{X}\mathbf{X}^\top \in \mathbb{R}^{n \times n}$, and follow the same steps to construct \mathbf{Q} and \mathbf{K} .

In the case that $\mathbf{Q} \in \mathbb{R}^d \times \mathbb{R}^{d_k}$ and $\mathbf{K} \in \mathbb{R}^d \times \mathbb{R}^{d_k}$ and $d_k > d$, we can use the same \mathbf{Q} and \mathbf{K} (Equations (19) and (21)) padded with zeros. We define the $\mathbf{Q}' \in \mathbb{R}^d \times \mathbb{R}^{d_{key}}$ and $\mathbf{K}' \in \mathbb{R}^d \times \mathbb{R}^{d_{key}}$ as follows:

$$\mathbf{Q}'_{i,j} = \begin{cases} \mathbf{Q}_{i,j} & j \leq d \\ 0 & \text{otherwise} \end{cases} \quad (30)$$

$$\mathbf{K}'_{i,j} = \begin{cases} \mathbf{K}_{i,j} & j \leq d \\ 0 & \text{otherwise} \end{cases} \quad (31)$$

□

B.1 DPGAT is strictly weaker than GATv2

There are examples of node representations that are linearly dependent and mappings φ , for which dynamic attention does not hold. First, we show a simple 2-dimensional example, and then we show the general case of such examples.

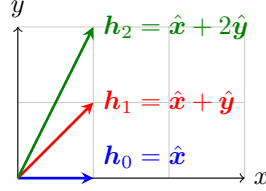


Figure 5: An example for node representations that are linearly dependent, for which DPGAT cannot compute dynamic attention, because no query vector $\mathbf{q} \in \mathbb{R}^2$ can “select” \mathbf{h}_1 .

Consider the following linearly dependent set of vectors $\mathbb{K} = \mathbb{Q}$ (Figure 5):

$$\mathbf{h}_0 = \hat{\mathbf{x}} \quad (32)$$

$$\mathbf{h}_1 = \hat{\mathbf{x}} + \hat{\mathbf{y}} \quad (33)$$

$$\mathbf{h}_2 = \hat{\mathbf{x}} + 2\hat{\mathbf{y}} \quad (34)$$

where $\hat{\mathbf{x}}$ and $\hat{\mathbf{y}}$ are the cartesian unit vectors. We define $\beta \in \{0, 1, 2\}$ to express $\{\mathbf{h}_0, \mathbf{h}_1, \mathbf{h}_2\}$ using the same expression:

$$\mathbf{h}_\beta = \hat{\mathbf{x}} + \beta\hat{\mathbf{y}} \quad (35)$$

Let $\mathbf{q} \in \mathbb{Q}$ be any query vector. For brevity, we define the unscaled dot-product attention score as s :

$$s(\mathbf{q}, \mathbf{h}_\beta) = e(\mathbf{q}, \mathbf{h}_\beta) \cdot \sqrt{d_k} \quad (36)$$

Where e is the attention score function of DPGAT (Equation (8)). The (unscaled) attention score between \mathbf{q} and $\{\mathbf{h}_0, \mathbf{h}_1, \mathbf{h}_2\}$ is:

$$s(\mathbf{q}, \mathbf{h}_\beta) = (\mathbf{q}^\top \mathbf{Q}) (\mathbf{h}_\beta^\top \mathbf{K})^\top \quad (37)$$

$$= (\mathbf{q}^\top \mathbf{Q}) \left((\hat{\mathbf{x}} + \beta\hat{\mathbf{y}})^\top \mathbf{K} \right)^\top \quad (38)$$

$$= (\mathbf{q}^\top \mathbf{Q}) (\hat{\mathbf{x}}^\top \mathbf{K} + \beta\hat{\mathbf{y}}^\top \mathbf{K})^\top \quad (39)$$

$$= (\mathbf{q}^\top \mathbf{Q}) (\hat{\mathbf{x}}^\top \mathbf{K})^\top + \beta (\mathbf{q}^\top \mathbf{Q}) (\hat{\mathbf{y}}^\top \mathbf{K})^\top \quad (40)$$

The first term $(\mathbf{q}^\top \mathbf{Q}) (\hat{\mathbf{x}}^\top \mathbf{K})^\top$ is unconditioned on β , and thus shared for every \mathbf{h}_β . Let us focus on the second term $\beta (\mathbf{q}^\top \mathbf{Q}) (\hat{\mathbf{y}}^\top \mathbf{K})^\top$. If $(\mathbf{q}^\top \mathbf{Q}) (\hat{\mathbf{y}}^\top \mathbf{K})^\top > 0$, then:

$$e(\mathbf{q}, \mathbf{h}_2) > e(\mathbf{q}, \mathbf{h}_1) \quad (41)$$

Otherwise, if $(\mathbf{q}^\top \mathbf{Q}) (\hat{\mathbf{y}}^\top \mathbf{K})^\top \leq 0$:

$$e(\mathbf{q}, \mathbf{h}_0) \geq e(\mathbf{q}, \mathbf{h}_1) \quad (42)$$

Thus, for any query \mathbf{q} , the key \mathbf{h}_1 can never get the highest score, and thus cannot be ‘‘selected’’. That is, the key \mathbf{h}_1 cannot satisfy that $e(\mathbf{q}, \mathbf{h}_1)$ is strictly greater than any other key.

In the general case, let $\mathbf{h}_0, \mathbf{h}_1 \in \mathbb{R}^d$ be some non-zero vectors, and λ is some scalar such that $0 < \lambda < 1$.

Consider the following linearly dependent set of vectors:

$$\mathbb{K} = \mathbb{Q} = \{\beta \mathbf{h}_1 + (1 - \beta) \mathbf{h}_0 \mid \beta \in \{0, \lambda, 1\}\} \quad (43)$$

For any query $\mathbf{q} \in \mathbb{Q}$ and $\beta \in \{0, \lambda, 1\}$ we define:

$$s(\mathbf{q}, \beta) = e(\mathbf{q}, (\beta \mathbf{h}_1 + (1 - \beta) \mathbf{h}_0)) \cdot \sqrt{d_k} \quad (44)$$

Where e is the attention score function of DPGAT (Equation (8)).

Therefore:

$$s(\mathbf{q}, \beta) = (\mathbf{q}^\top \mathbf{Q}) \left((\beta \mathbf{h}_1 + (1 - \beta) \mathbf{h}_0)^\top \mathbf{K} \right)^\top \quad (45)$$

$$= (\mathbf{q}^\top \mathbf{Q}) (\beta \mathbf{h}_1^\top \mathbf{K} + (1 - \beta) \mathbf{h}_0^\top \mathbf{K})^\top \quad (46)$$

$$= (\mathbf{q}^\top \mathbf{Q}) (\beta \mathbf{h}_1^\top \mathbf{K} + \mathbf{h}_0^\top \mathbf{K} - \beta \mathbf{h}_0^\top \mathbf{K})^\top \quad (47)$$

$$= (\mathbf{q}^\top \mathbf{Q}) (\beta (\mathbf{h}_1^\top \mathbf{K} - \mathbf{h}_0^\top \mathbf{K}) + \mathbf{h}_0^\top \mathbf{K})^\top \quad (48)$$

$$= \beta (\mathbf{q}^\top \mathbf{Q}) (\mathbf{h}_1^\top \mathbf{K} - \mathbf{h}_0^\top \mathbf{K})^\top + (\mathbf{q}^\top \mathbf{Q}) (\mathbf{h}_0^\top \mathbf{K})^\top \quad (49)$$

If $(\mathbf{q}^\top \mathbf{Q}) (\mathbf{h}_1^\top \mathbf{K} - \mathbf{h}_0^\top \mathbf{K})^\top > 0$:

$$e(\mathbf{q}, \mathbf{h}_1) > e(\mathbf{q}, \mathbf{h}_\lambda) \quad (50)$$

Otherwise, if $(\mathbf{q}^\top \mathbf{Q}) (\mathbf{h}_1^\top \mathbf{K} - \mathbf{h}_0^\top \mathbf{K})^\top \leq 0$:

$$e(\mathbf{q}, \mathbf{h}_0) \geq e(\mathbf{q}, \mathbf{h}_\lambda) \quad (51)$$

Thus, for any query \mathbf{q} , the key \mathbf{h}_λ cannot be selected. That is, the key \mathbf{h}_λ cannot satisfy that $e(\mathbf{q}, \mathbf{h}_\lambda)$ is strictly greater than any other key. Therefore, there are mappings φ , for which dynamic attention does not hold.

While we prove that GATv2 computes dynamic attention (Appendix A) for *any* set of node representations $\mathbb{K} = \mathbb{Q}$, there are sets of node representations and mappings φ for which dynamic attention does not hold for DPGAT. Thus, DPGAT is strictly weaker than GATv2.

C Complexity Analysis

We repeat the definitions of GAT, GATv2 and DPGAT:

$$\text{GAT (Veličković et al., 2018):} \quad e(\mathbf{h}_i, \mathbf{h}_j) = \text{LeakyReLU}(\mathbf{a}^\top \cdot [\mathbf{W} \mathbf{h}_i \parallel \mathbf{W} \mathbf{h}_j]) \quad (52)$$

$$\text{GATv2 (our fixed version):} \quad e(\mathbf{h}_i, \mathbf{h}_j) = \mathbf{a}^\top \text{LeakyReLU}(\mathbf{W} \cdot [\mathbf{h}_i \parallel \mathbf{h}_j]) \quad (53)$$

$$\text{DPGAT (Vaswani et al., 2017):} \quad e(\mathbf{h}_i, \mathbf{h}_j) = \left((\mathbf{h}_i^\top \mathbf{Q}) \cdot (\mathbf{h}_j^\top \mathbf{K})^\top \right) / \sqrt{d'} \quad (54)$$

C.1 Time Complexity

GAT As noted by Veličković et al. (2018), the time complexity of a single GAT head may be expressed as $\mathcal{O}(|\mathcal{V}|dd' + |\mathcal{E}|d')$. Because of GAT’s static attention, this computation can be further optimized, by merging the linear layer \mathbf{a}_1 with \mathbf{W} , merging \mathbf{a}_2 with \mathbf{W} , and only then compute $\mathbf{a}_{\{1,2\}}^\top \mathbf{W} \mathbf{h}_i$ for every $i \in \mathcal{V}$.

GATv2 require the same computational cost as GAT’s declared complexity: $\mathcal{O}(|\mathcal{V}|dd' + |\mathcal{E}|d')$: we denote $\mathbf{W} = [\mathbf{W}_1 \| \mathbf{W}_2]$, where $\mathbf{W}_1 \in \mathbb{R}^{d' \times d}$ and $\mathbf{W}_2^{d' \times d}$ contain the left half and right half of the columns of \mathbf{W} , respectively. We can first compute $\mathbf{W}_1 \mathbf{h}_i$ and $\mathbf{W}_2 \mathbf{h}_j$ for every $i, j \in \mathcal{V}$. This takes $\mathcal{O}(|\mathcal{V}|dd')$.

Then, for every edge (j, i) , we compute $\text{LeakyReLU}(\mathbf{W} \cdot [\mathbf{h}_i \| \mathbf{h}_j])$ using the precomputed $\mathbf{W}_1 \mathbf{h}_i$ and $\mathbf{W}_2 \mathbf{h}_j$, since $\mathbf{W} \cdot [\mathbf{h}_i \| \mathbf{h}_j] = \mathbf{W}_1 \mathbf{h}_i + \mathbf{W}_2 \mathbf{h}_j$. This takes $\mathcal{O}(|\mathcal{E}|d')$.

Finally, computing the results of the linear layer \mathbf{a} takes additional $\mathcal{O}(|\mathcal{E}|d')$ time, and overall $\mathcal{O}(|\mathcal{V}|dd' + |\mathcal{E}|d')$.

DPGAT also takes the same time. We can first compute $\mathbf{h}_i^\top \mathbf{Q}$ and $\mathbf{h}_j^\top \mathbf{K}$ for every $i, j \in \mathcal{V}$. This takes $\mathcal{O}(|\mathcal{V}|dd')$. Computing the dot-product $(\mathbf{h}_i^\top \mathbf{Q})(\mathbf{h}_j^\top \mathbf{K})^\top$ for every edge (j, i) takes additional $\mathcal{O}(|\mathcal{E}|d')$ time, and overall $\mathcal{O}(|\mathcal{V}|dd' + |\mathcal{E}|d')$.

C.2 Parametric Complexity

	GAT	GATv2	DPGAT
Official	$2d' + dd'$	$d' + 2dd'$	$2dd_k + dd'$
In our experiments	$2d' + dd'$	$d' + dd'$	$2dd'$

Table 5: Number of parameters for each GNN type, in a single layer and a single attention head.

All parametric costs are summarized in Table 5. All following calculations refer to a single layer having a single attention head, omitting bias vectors.

GAT has learned vector and a matrix: $\mathbf{a} \in \mathbb{R}^{2d'}$ and $\mathbf{W} \in \mathbb{R}^{d' \times d}$, thus overall $2d' + dd'$ learned parameters.

GATv2 has a matrix that is twice larger: $\mathbf{W} \in \mathbb{R}^{d' \times 2d}$, because it is applied on the concatenation $[\mathbf{h}_i \| \mathbf{h}_j]$. Thus, the overall number of learned parameters is $d' + 2dd'$. However in our experiments, to rule out the increased number of parameters over GAT as the source of empirical difference, we constrained $\mathbf{W} = [\mathbf{W}' \| \mathbf{W}']$, and thus the number of parameters were $d' + dd'$.

DPGAT has \mathbf{Q} and \mathbf{K} matrices of sizes dd_k each, and additional dd' parameters in the value matrix \mathbf{V} , thus $2dd_k + dd'$ parameters overall. However in our experiments, we constrained $\mathbf{Q} = \mathbf{K}$ and set $d_k = d'$, and thus the number of parameters is only $2dd'$.

D Training details

In this section we elaborate on the training details of all of our experiments. All used code and data are publicly available under the MIT license.

D.1 Node- and Link-Prediction

We used the provided splits of OGB (Hu et al., 2020) and the Adam optimizer. We tuned the following hyperparameters: number of layers $\in \{2, 3, 6\}$, hidden size $\in \{64, 128, 256\}$, learning rate $\in \{0.0005, 0.001, 0.005, 0.01\}$ and sampling method – full batch, GraphSAINT (Zeng et al., 2019) and NeighborSampling (Hamilton et al., 2017). We tuned hyperparameters according to validation score and early stopping. The final hyperparameters are detailed in Table 6.

Dataset	# layers	Hidden size	Learning rate	Sampling method
ogbn-arxiv	3	256	0.01	GraphSAINT
ogbn-products	3	128	0.001	NeighborSampling
ogbn-mag	2	256	0.01	NeighborSampling
ogbn-proteins	6	64	0.01 (GAT, GATv2) 0.001 (DPGAT)	NeighborSampling
ogbl-collab	3	64	0.001	Full Batch
ogbl-citation2	3	256	0.0005	NeighborSampling

Table 6: Training details of node- and link-prediction datasets.

D.2 Robustness to Noise

In these experiments, we used the same best-found hyperparameters in node-prediction, with 8 attention heads in **ogbn-arxiv** and 1 head in **ogbn-mag**. Each point is an average of 10 runs.

D.3 Synthetic Benchmark: DICTIONARYLOOKUP

In all experiments, we used a learning rate decay of 0.5, a hidden size of $d = 128$, a batch size of 1024, and the Adam optimizer.

We created a separate dataset for every graph size (k), and we split each such dataset to train and test with a ratio of 80:20. Since this is a contrived problem, we did not use a validation set, and the reported test results can be thought of as validation results. Every model was trained on a fixed value of k . Every key node (bottom row in Figure 2) was encoded as a sum of learned attribute embedding and a value embedding, followed by ReLU.

We experimented with layer normalization, batch normalization, dropout, various activation functions and various learning rates. None of these changed the general trend, so the experiments in Figure 3 were conducted without any normalization, without dropout and a learning rate of 0.001.

D.4 Programs: VARMISSUSE

We used the code, splits, and the same best-found configurations as Brockschmidt (2020), who performed an extensive hyperparameter tuning by searching over 30 configurations for each GNN type. We trained each model five times.

We took the best-found hyperparameters of Brockschmidt (2020) for GAT and used them to train GATv2 and DPGAT, without any further tuning.

D.5 Graph-Prediction: QM9

We used the code and splits of Brockschmidt (2020) who performed an extensive hyperparameter search over 500 configurations. We took the best-found hyperparameters of Brockschmidt (2020) for GAT and used them to train GATv2 and DPGAT. The only minor change from GAT is placing a residual connection after every layer, rather than after every other layer, which is within the experimented hyperparameter search that was reported by Brockschmidt (2020).

E Data Statistics

E.1 Node- and Link-Prediction Datasets

Statistics of the OGB datasets we used for node- and link-prediction are shown in Table 7.

E.2 QM9

Statistics of the QM9 dataset, as used in Brockschmidt (2020) are shown in Table 8.

Dataset	# nodes	# edges	Avg. node degree	Diameter
ogbn-arxiv	169,343	1,166,243	13.7	23
ogbn-mag	1,939,743	21,111,007	21.7	6
ogbn-products	2,449,029	61,859,140	50.5	27
ogbn-proteins	132,534	39,561,252	597.0	9
ogbl-collab	235,868	1,285,465	8.2	22
ogbl-citation2	2,927,963	30,561,187	20.7	21

Table 7: Statistics of the OGB datasets (Hu et al., 2020).

	Training	Validation	Test
# examples	110,462	10,000	10,000
# nodes - average	18.03	18.06	18.09
# edges - average	18.65	18.67	18.72
Diameter - average	6.35	6.35	6.35

Table 8: Statistics of the QM9 chemical dataset (Ramakrishnan et al., 2014) as used by Brockschmidt (2020).

E.3 VARMISUSE

Statistics of the VARMISUSE dataset, as used in Allamanis et al. (2018) and Brockschmidt (2020), are shown in Table 9.

	Training	Validation	UnseenProject Test	SeenProject Test
# graphs	254360	42654	117036	59974
# nodes - average	2377	1742	1959	3986
# edges - average	7298	7851	5882	12925
Diameter - average	7.88	7.88	7.78	7.82

Table 9: Statistics of the VARMISUSE dataset (Allamanis et al., 2018) as used by Brockschmidt (2020).

F Additional Results

F.1 DICTIONARYLOOKUP

Figure 6 shows additional comparison between GATv2 and GIN (Xu et al., 2019) in the DICTIONARYLOOKUP problem. GATv2 easily achieves 100% train and test accuracy even for $k=100$ and using only a single head. GIN, although considered as more expressive than other GNNs, cannot perfectly fit the training data (with a model size of $d = 128$) starting from $k=20$.

F.2 QM9

Standard deviation for the QM9 results of Section 4.6 are presented in Table 10.

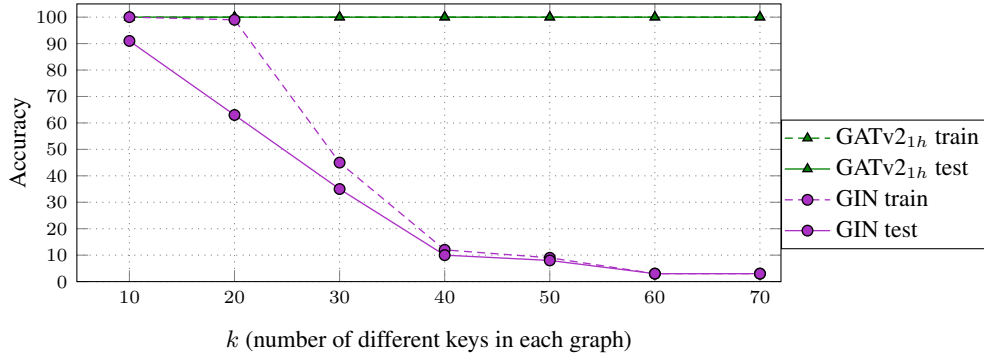


Figure 6: Train and test accuracy across graph sizes in the DICTIONARYLOOKUP problem. GATv2 easily achieves 100% train and test accuracy even for $k=100$ and using only a single head. GIN (Xu et al., 2019), although considered as more expressive than other GNNs, cannot perfectly fit the training data (with a model size of $d = 128$) starting from $k=20$.

Model	Predicted Property						
	1	2	3	4	5	6	7
GCN [†]	3.21±0.06	4.22 ±0.45	1.45±0.01	1.62±0.04	2.42±0.14	16.38±0.49	17.40±3.56
GIN [†]	2.64±0.11	4.67±0.52	1.42±0.01	1.50±0.09	2.27±0.09	15.63 ±1.40	12.93±1.81
GAT _{1h}	3.08±0.08	7.82±1.42	1.79±0.10	3.96±1.51	3.58±1.03	35.43±29.9	116.5±10.65
DPGAT _{1h}	3.20±0.17	8.35±0.78	1.71±0.03	2.17±0.14	2.88±0.12	25.21±2.86	65.79±39.84
GATv2 _{1h}	3.04±0.06	6.38±0.62	1.68±0.04	2.18±0.61	2.82±0.25	20.56±0.70	77.13±37.93
GAT _{8h} [†]	2.68±0.06	4.65±0.44	1.48±0.03	1.53±0.07	2.31±0.06	52.39±42.58	14.87±2.88
DPGAT _{8h}	2.63 ±0.09	4.37±0.13	1.44±0.07	1.40 ±0.03	2.10 ±0.07	32.59±34.77	11.66 ±1.00
GATv2 _{8h}	2.65±0.05	4.28±0.27	1.41 ±0.04	1.47±0.03	2.29±0.15	16.37±0.97	14.03±1.39

Model	Predicted Property						Rel. to GAT _{8h}
	8	9	10	11	12	13	
GCN [†]	7.82±0.80	8.24±1.25	9.05±1.21	7.00±1.51	3.93±0.48	1.02 ±0.05	-1.5%
GIN [†]	5.88 ±1.01	18.71±23.36	5.62 ±0.81	5.38 ±0.75	3.53 ±0.37	1.05±0.11	-2.3%
GAT _{1h}	28.10±16.45	20.80±13.40	15.80±5.87	10.80±2.18	5.37±0.26	3.11±0.14	+134.1%
DPGAT _{1h}	12.93±1.70	13.32±2.39	14.42±1.95	13.83±2.55	6.37±0.28	3.28±1.16	+77.9%
GATv2 _{1h}	10.19±0.63	22.56±17.46	15.04±4.58	22.94±17.34	5.23±0.36	2.46±0.65	+91.6%
GAT _{8h} [†]	7.61±0.46	6.86±0.53	7.64±0.92	6.54±0.36	4.11±0.27	1.48±0.87	+0%
DPGAT _{8h}	6.95±0.32	7.09±0.59	7.30±0.66	6.52±0.61	3.76±0.21	1.18±0.33	-9.7%
GATv2 _{8h}	6.07±0.77	6.28 ±0.83	6.60±0.79	5.97±0.94	3.57±0.36	1.59±0.96	-11.5%

Table 10: Average error rates (lower is better), 5 runs ± standard deviation for each property, on the QM9 dataset. † was previously tuned and reported by Brockschmidt (2020).